J. Fluid Mech. (1994), *vol.* 278, *pp.* 83–100

The evolution and bifurcation of a pendant drop

By R. M. S. M. SCHULKES
School of Mathematics, University of East Anglia, Norwich NR4 7TJ, UK

(Received 2 February 1994 and in revised form 23 May 1994)

In this paper we calculate how a pendant drop evolves at the end of a nozzle when the volume of the drop increases steadily with time. We find that the character of the evolution is strongly dependent on the growth rate of the drop and the radius of the nozzle. Typically we find that once the drop has become unstable, two bifurcations occur shortly after each other when the growth rate of the drop is slow. For large growth rates the bifurcations are well-separated in time. We are able to calculate the volumes of the drops after the bifurcations. A comparison with experimental data shows a satisfactory agreement.

1. Introduction

Many people, at some time, will have observed the formation of a pendant drop at the end of a tap. One sees that the drop grows slowly at first but the evolution speeds up once the drop has grown beyond a certain size. The evolution of the drop close to the breaking point is very rapid indeed so that intricate details of the very complex bifurcation behaviour are almost impossible to discern with the naked eye. It is however possible to see that usually not just one drop breaks away: besides the main drop there is often a small secondary drop. The presence of this secondary drop was remarked upon by Guthrie (1863) and Worthington (1881), but it was not until high-speed camera equipment was developed that the full details of the bifurcation process could be observed. One of the first sequences of photographs, showing details of the bifurcation process and the effect of viscosity on the bifurcation behaviour, was published by Hauser *et al.* (1936). More recently, a very clear sequence of photographs showing details of the bifurcation was published by Peregrine, Shoker & Symon (1990). These photographs show that immediately prior to the bifurcation, the fluid region consists of an almost spherical drop connected through a thin liquid bridge to a conically shaped region. A bifurcation occurs first at the point at which the liquid bridge is connected to the drop. Subsequently, the drop descends and large undulations form on the liquid bridge as a result of the recoil following the bifurcation. Eventually a secondary bifurcation occurs on the liquid bridge, resulting in the formation of a satellite drop. This satellite drop has a much smaller volume than the main drop.

Experimental measurements have shown that the volume of fluid which breaks away from the point of attachment of the drop is significantly less than the critical volume for which the drop is just stable. Of the total volume of a pendant drop, as little as half may break away. Early experiments to measure the volume of a drop falling from the tip of a pipette were carried out by Tate (1864) and Rayleigh (1899). Later, Harkins & Brown (1919) carried out very careful and precise experiments on drop volumes with the aim to infer the coefficient of surface tension from the volume of the drop. It is important to note that in all experimental determinations of drop volumes, the total volume of fluid breaking away from the point of attachment, that is the combined volumes of the main drop and the satellite drop, is measured.

Attempts to obtain a theoretical estimate of the actual volume which has broken away are severely hampered by the fact that after the stability boundary has been passed, the fluid domain undergoes enormous deformations before the bifurcation actually occurs. It is clear that linear theories are not applicable in this unstable regime. Besides some asymptotic work on idealized problems by Ting & Keller (1990), it appears that the evolution of a pendant drop close to the bifurcation point has only recently been studied, by Eggers (1993) and Eggers & Dupont (1994). Eggers (1993) uses an expansion of the Navier–Stokes equations in the radial coordinate to study the self-similar behaviour of the necking region. To model the evolution of the complete pendant drop as the bifurcation point is approached, Eggers & Dupont (1994) solve (by numerical means) the equations derived by Eggers (1993). A qualitative comparison of these calculations with the photographs by Peregrine *et al.* (1990) yields a good agreement. This agreement is truly remarkable when one realizes that that Eggers' model essentially constitutes a long-wavelength approximation of the Navier–Stokes equations. Implicit in this model is the assumption that variations in the axial direction occur on a lengthscale which is long compared with a typical radial lengthscale. This assumption is certainly not satisfied in the calculations presented by Eggers & Dupont (1994). Schulkes (1993) has investigated the accuracy of various one-dimensional models for inviscid fluids. He found that the one-dimensional model of Lee (1974), which is identical to Eggers' model when viscous effects are neglected, is only accurate when gradients of the free surface are small. Furthermore, Lee's model was found to be highly unstable as soon as short-wavelength effects (such as large gradients) became important. No instabilities are mentioned in the calculations by Eggers & Dupont (1994) even though the gradient of the free surface is formally infinite at the point at which the free surface intersects the symmetry axis. The inclusion of the viscous term by Eggers & Dupont (1994) evidently leads to a model with improved accuracy and stability characteristics.

Besides the obvious difficulties of dealing with a highly nonlinear free-boundary problem, the bifurcating drop problem has the added difficulty that one is faced with the singularity in the governing equations at the bifurcation point. The singularity stems from the fact that the curvature tends to infinity as the bifurcation point is approached. It will be evident that the large local value of the curvature close to the bifurcation point makes the actual bifurcation a violent process. If it were possible to continue the calculation beyond the bifurcation point one would be faced with a secondary bifurcation leading to the satellite drop as indicated above. Following this secondary bifurcation one is left with a conical fluid region. An idea of how this fluid cone evolves can be obtained from the study of Keller & Miksis (1983) on the evolution of a two-dimensional fluid wedge. They showed that the evolution of the fluid wedge is self-similar in character and its seems likely that a similar result may hold for the axisymmetric case.

From the above considerations it is clear that the bifurcation process of a pendant drop can be divided into three stages. First, the pendant drop grows until a bifurcation occurs, resulting in the formation of the main drop. Subsequently, undulations form on a fluid filament, possibly resulting in a secondary bifurcation thereby producing the satellite drop. After the secondary bifurcation a cone-shaped fluid region is left which contracts in some unknown manner. In this paper we study these three stages of the evolution process of the unstable pendant drop. Potential flow conditions are assumed and a boundary integral method is used to solve the nonlinear free-boundary problem numerically. We investigate how the evolution of the drop is affected by the rate at which the drop grows and by the radius of the tube at which the drop forms. We are

able to continue the calculation until close to the bifurcation point thereby enabling us to calculate the volume of the drops after bifurcation. Special treatment of the free surface in the necking region allows us to continue the calculation beyond the bifurcation point. These calculations show the formation of a satellite drop quite similar to that observed in experiments. A comparison of drop volumes obtained experimentally with those obtained in our calculations, shows a satisfactory agreement.

2. Governing equations

The governing equations are derived under the important assumptions that the fluid is incompressible and that viscous effects are negligible. Under the additional assumption that the fluid flow is irrotational, it is well-known that the motion of such a fluid is given in terms of a velocity potential which satisfies Laplace's equation. In order to simplify the problem still further we assume that the problem is axisymmetric, i.e. the velocity potential ϕ is independent of the azimuthal coordinate. Laplace's equation for ϕ reads therefore

$$\frac{\partial^2\phi}{\partial r^2}+\frac{1}{r}\frac{\partial\phi}{\partial r}+\frac{\partial^2\phi}{\partial z^2}=0. \tag{1}$$

On the capillary surface three boundary conditions are given. The two kinematic conditions are

$$\frac{\mathrm{D}r}{\mathrm{D}t}=\frac{\partial\phi}{\partial r}=n_r\frac{\partial\phi}{\partial n}-n_z\frac{\partial\phi}{\partial s}, \quad \frac{\mathrm{D}z}{\mathrm{D}t}=\frac{\partial\phi}{\partial z}=n_z\frac{\partial\phi}{\partial n}+n_r\frac{\partial\phi}{\partial s}, \tag{2}$$

and the dynamic condition reads

$$\frac{\mathrm{D}\phi}{\mathrm{D}t}=\tfrac{1}{2}|\nabla\phi|^2+\frac{1}{R_1}+\frac{1}{R_2}+p_0-Bo\,z. \tag{3}$$

In the above equations $\mathrm{D}/\mathrm{D}t=\partial/\partial t+(\nabla\phi\cdot\nabla)$ denotes a Lagrangian time derivative, (n_r, n_z) is a unit normal to the capillary surface, R_1 and R_2 are the principal radii of curvature of the free surface and p_0 a pressure constant which is defined by the equations governing the static surface. The equations have been made dimensionless by taking the radius of the nozzle at which the drop forms as the typical lengthscale and the capillary timescale is equal to $T=(\rho R^3/\sigma)^{1/2}$. The dimensionless number which appears is the Bond number defined as $Bo=\rho g R^2/\sigma$. We assume that initially the free surface is flat, situated at the mouth of the nozzle which points vertically downwards. The nozzle is taken to be of unit (dimensionless) length, the mouth is situated at $z=-1$, and on the nozzle inlet at $z=0$ some volume flux is prescribed. It is assumed that at $t=0$ the whole system is at rest so that the pressure constant is given by $p_0=-Bo$. The rim of the nozzle is assumed to be sharp so that no contact-angle condition needs to be satisfied on the curve at which the free surface intersects the nozzle. By assuming a sharp-rimmed nozzle we implicitly impose the condition that the free surface remains fixed to the rim of the nozzle at all times. The sides of the nozzle at $r=1$ are assumed impermeable so that on the nozzle boundary we have

$$\left.\frac{\partial\phi}{\partial r}\right|_{r=1}=0. \tag{4}$$

On the nozzle inlet we assume that for $t>0$ the flux is of the form

$$\left.\frac{\partial\phi}{\partial z}\right|_{z=0}=We^{1/2}\psi(r), \tag{5}$$

where $We = V^2\rho R/\sigma$ is the Weber number (V is a typical fluid velocity at the nozzle inlet) and $\psi(r)$ is some prescribed flux. We shall find it convenient to present results in terms of the dimensionless volume flux rather than the Weber number. The dimensionless volume flux $\mathcal{Q}$ is the volume of fluid passing through $z = 0$ per unit time. Hence, with $\psi(r) = r - 1$ we obtain

$$\mathcal{Q} = -2\pi \int_0^1 \left.\frac{\partial \phi}{\partial z}\right|_{z=0} r\,dr = \pi We^{1/2}/3.$$

Note that not every function $\psi(r)$ is admissible since we require that the velocity field entering the nozzle through $z = 0$ should be irrotational. The velocity field generated by the potential $\phi = (r-1)z$ of course satisfies this requirement.

It is important to realize that there are essentially two timescales associated with the drop problem. The capillary timescale T defined earlier is the relevant timescale for surface-tension-governed dynamic effects. However, given the volume flux through the mouth of the nozzle, we find that a drop develops on a timescale $\tau = R/V \sim T/\mathcal{Q}$. Clearly $\tau \sim T$ only when $\mathcal{Q} \sim O(1)$. When $\mathcal{Q} \ll 1$ changes of the free surface shape are generally small on the capillary timescale T. Eventually the drop will become unstable, after which significant changes will occur on the capillary timescale. Hence, since the main aim of this study is to investigate the evolution process in the unstable regime, we have chosen to take T as the relevant timescale.

The problem outlined in (1)–(5) is of the free-boundary type with the capillary surface undergoing large deformations. For this reason it is beneficial to use the integral equivalent of (1) which leads to a one-dimensional problem defined only on the curve bounding the fluid domain in the (r, z)-plane. Hence, given the Green's function for the Laplace equation in an axisymmetric geometry, the integral equation which is obtained after application of Green's theorem and the boundary conditions (4) and (5) is an integral equation of the first kind for the flux on the free surface. The movement of the free surface is governed by the two kinematic conditions (1) while the dynamic condition (2) prescribes the velocity potential on the free surface. The given equations can only be solved numerically owing to the highly nonlinear character of the evolution of the free surface. All details of the numerical approximations and time integration are omitted; a discussion of numerical aspects can be found in Schulkes (1994) in which a closely related problem was studied. We just mention that extensive regridding is used during the time integration in order to control the position of the nodes on the free surface. Nodes are relocated after each time step in the numerical integration such that the nodal separation is inversely proportional to the local curvature of the surface. This has the effect that regions of the surface which are strongly curved have a dense distribution of nodes and vice versa.

3. Behaviour close to the bifurcation point

As was pointed out earlier, the evolution of the drop is such that after a finite time a physical bifurcation of the fluid domain occurs. This bifurcation is the result of the fact that for a given nozzle, there is a maximum volume for which the drop is stable, see Padday & Pitt (1973). Allowing the volume of the drop to increase beyond this maximum leads to the bifurcation whereby a part of the fluid domain breaks away from the nozzle. For this bifurcation to occur, a necking region has to form at some point in the fluid domain, the bifurcation point being the point at which the radius of the neck vanishes. Denoting the radius of the neck by R_n, it follows that the curvature in the necking region is $O(1/R_n)$. Hence, the surface force (which is proportional to the

local curvature) tends to infinity as the radius of the neck tends to zero. It should not be surprising, therefore, that severe numerical difficulties are experienced as the bifurcation point is approached. For this reason the radius of the neck is not allowed to decrease below the value $R_n = 0.02$. This is an arbitrary condition only motivated by the fact that numerical instabilities are experienced when the radius is allowed to decrease further. Generally, instabilities would occur within 5 time steps (with $\Delta t \leqslant 0.01$) after the minimum radius of the neck was allowed to decrease below the value 0.02. It should be pointed out that the nature of the instabilities is entirely numerical. With a fixed time step the increased acceleration of the neck would lead to an 'overshoot' of the necking radius: the radius would become negative. Relating the time step to the radius of the neck (thereby decreasing the time step as the bifurcation point is approached) would only delay difficulties: eventually a floating point exception would occur once the radius had decreased sufficiently. These results do no exclude the possibility that other instabilities, which may be inherent in the model as the bifurcation point is approached, are present. However, within the resolution of our code there was no evidence of such instabilities.

Recently, Oğuz & Prosperetii (1993) studied the problem of the detachment of a bubble from a needle in which a bifurcation similar to that outlined above occurs. They solved the difficulties associated with the bifurcation by allowing the neck to decrease to no further than 10% of the radius of the needle. The free surface was then joined to the symmetry axis by means of a circular arc under the assumption that the potential along the arc is constant. We find this approach somewhat unsatisfactory since it significantly reduces the strong recoil resulting from the large values of the curvature in the necking region. Therefore the following procedure is adopted in our calculations. Consider the free-surface configuration as depicted in figure 1 which is a typical configuration in the necking region when the calculation is terminated. Assume that the node closest to the symmetry axis has coordinates $(\Delta r, z)$ with $\Delta r = R_n < 0.02$. We now move the node located at $(\Delta r, z)$ onto the symmetry axis (cf. figure 1) and the value of the velocity potential on the symmetry axis is approximated via

$$\phi(0, z) = \phi(\Delta r, z) - \Delta r \left.\frac{\partial \phi}{\partial r}\right|_{(\Delta r, z)} + O(\Delta r^2).$$

Note that both ϕ and $\partial\phi/\partial r$ are known at the point $(\Delta r, z)$. Following the bifurcation, the fluid region below the bifurcation point (essentially the drop breaking away from the nozzle) is no longer incorporated in the calculation. The calculation is continued with just the fluid region connected to the nozzle.

The procedure outlined above completely ignores the intricate motion of the neck in a Δr-neighbourhood of the bifurcation point. However, there is reason to believe that this approximation affects the dynamics only on very short time- and lengthscales. Namely, the tip of the fluid cone which is formed by moving the surface node onto the symmetry axis has a curvature $O(1/\Delta r)$ so that the pressure in the tip of the cone is also $O(1/\Delta r)$. In the tip the pressure is balanced by the rate of change of the velocity potential, thus $\partial\phi/\partial t \sim \sigma/\Delta r$. Therefore, if ϕ changes over a lengthscale Δr the relevant timescale for $O(\Delta r)$-changes in ϕ is given by $\hat{t} \sim (\Delta r^3/\sigma)^{1/2}$. It follows that $O(\Delta r)$-changes in ϕ occur only on short timescales. On longer time- and lengthscales the details of the motion near the bifurcation point are unlikely to have a significant effect.

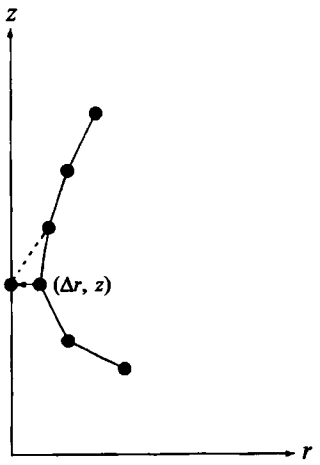

FIGURE 1. Schematic diagram of the necking region.

4. Examples of calculations

As a first example we take the case in which $Bo = 1$ and $\mathcal{Q} = 0.01$. The free-surface shapes during different stages of the evolution are shown in figures 2(*a*) and 2(*b*), before and after the bifurcation respectively. The dimensionless times at which the free-surface shapes are shown are indicated in the plots. Let us consider the dynamics prior to the bifurcation in some detail. We observe that the initial stage of the evolution is very slow with a drop slowly developing at the mouth of the nozzle. For such a slow growth rate it is fair to assume that the shapes of the drop at different stages during the evolution are closely approximated by the shapes of static pendant drops with corresponding volumes. As long as the volume of the drop is less than the critical volume (being the maximum volume for which the drop is stable), the drop will continue to evolve slowly. However, once the critical volume is exceeded the drop will become unstable and the evolution will speed up. The dimensionless critical volume when $Bo = 1$ is equal to $V_{crit} = 5.26$ (see Padday & Pitt 1973). For the given volume flux $\mathcal{Q} = 0.01$ this volume is reached at a time $t_{crit} = V_{crit}/\mathcal{Q} = 526$ and hence for $t > t_{crit}$ we expect an increasingly rapid evolution of the drop. This is exactly what is observed in figure 2(*a*). We see that during the final stages of the evolution before the bifurcation, a spherical drop is formed which is connected via a thin liquid bridge to a conical region with almost straight sides.

It was found that the point at which necking occurred was situated immediately above the spherical drop. To explain why the bifurcation occurred precisely at this point, we note that the pressure in the fluid region is roughly proportional to the curvature of the capillary surface. This implies that in the conical region above and the spherical region below the liquid bridge, the pressure is significantly lower than inside the liquid bridge. Hence, fluid will be squeezed out of the liquid bridge. The point at which the pressure gradient is largest corresponds to the region at which the curvature of the capillary surface changes most rapidly which, in turn, is also the point at which the volume flux out of the liquid bridge is largest. Clearly, the change in curvature of the surface is largest at the point at which the liquid bridge is connected to the spherical drop. Bifurcation will therefore occur at this point first rather than at the connection point between the conical region and the liquid bridge.

Since we are able to continue the calculation until close to the bifurcation point, it

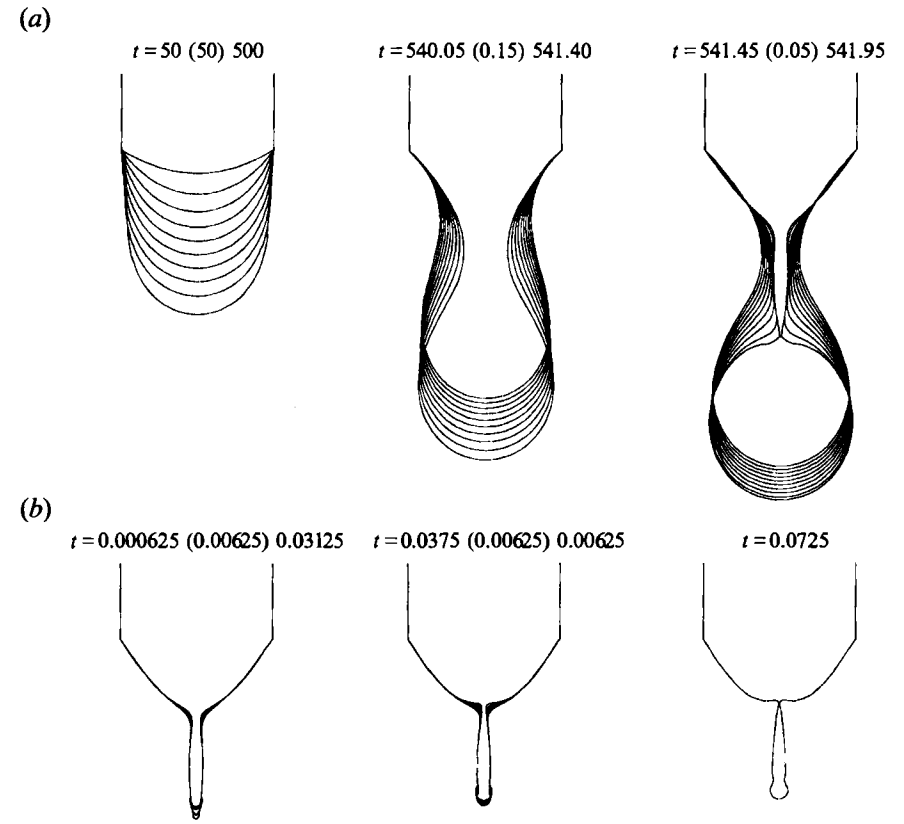

FIGURE 2. Plots of the free-surface shapes of the pendant drop during different stages of the evolution, (*a*) before and (*b*) after, the bifurcation. The Bond number is $Bo = 1$ and the discharge rate is $\mathcal{Q} = 0.01$.

is possible to calculate the volume of the fluid region below the bifurcation point. It was found that the volume of the spherical drop was equal to $V_1 = 3.93$ (the volume of fluid breaking away after the ith bifurcation will henceforth be denoted by V_i).

Following the bifurcation we observe (figure 2*b*) that the tip of the liquid filament retracts. The tip of the filament develops into a bulbous region and undulations form on the liquid filament as the bulbous tip moves upwards. At the same time we note that at the point where the liquid filament is connected to the conical region, a neck develops. The reason why the neck forms in that particular place is essentially the same as the reason why the neck prior to the first bifurcation occurred immediately above the spherical drop: the pressure gradient is largest at the point at which the filament is connected to the cone. The secondary bifurcation leads to the formation of the satellite drop and it is clear that the volume of the satellite drop is much smaller than that of the main drop. In fact, we find $V_2 = 0.022$ so that the volume of the satellite drop is less than 1% of the volume of the main drop.

Numerical experiments show that increasing the volume flux to $\mathcal{Q} = 0.1$ does not lead to significant qualitative changes in the evolution of the drop as compared with the case in which $\mathcal{Q} = 0.01$. However, a significant change occurs when the volume flux is increased to $\mathcal{Q} = 1$. The evolution of the drop for the parameters $Bo = 1$ and $\mathcal{Q} = 1$ is shown in figures 3(*a*) and 3(*b*), before and after the bifurcation respectively. We observe (figure 3*a*) that the volume flux is now so large that the slender liquid bridge

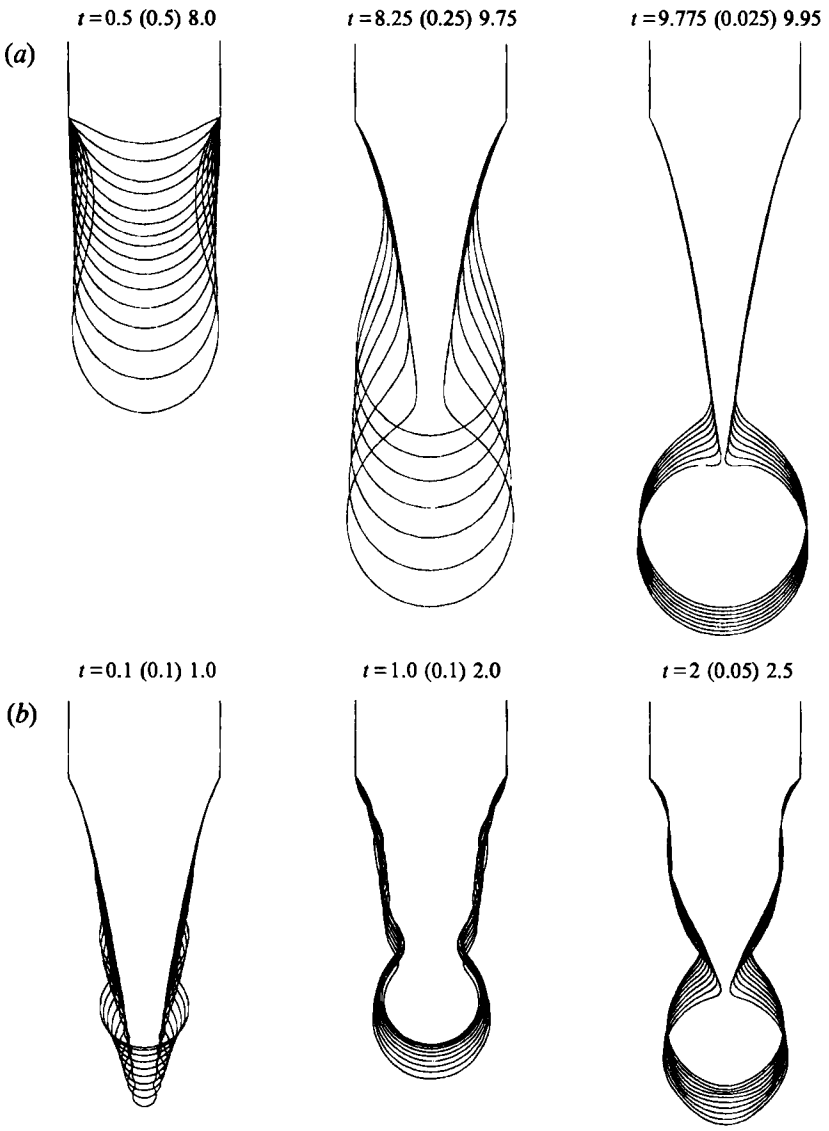

FIGURE 3. Plots of the free-surface shapes of the pendant drop during different stages of the evolution, (*a*) before and (*b*) after, the bifurcation. The Bond number is $Bo = 1$ and the discharge rate is $\mathcal{Q} = 1.0$.

seen in the previous case is no longer present. The fluid emerging from the nozzle is forced into the fluid region above the bifurcation point thereby producing a long liquid cone which connects the nozzle to the drop. As before, the bifurcation occurs immediately above the spherical drop, which has the volume $V_1 = 6.33$. Note that this drop volume is significantly larger than the drop volume in the case with $\mathcal{Q} = 0.01$. Following the bifurcation we see (figure 3*b*) that at first the tip of the liquid cone retracts upwards and develops the bulbous region seen in the case with $\mathcal{Q} = 0.01$. However, owing to the continued ejection of fluid from the nozzle the tip of the distorted cone reaches a maximum height and starts to descend. As it does so, the bulbous head continues to expand and a neck starts to develop behind the head.

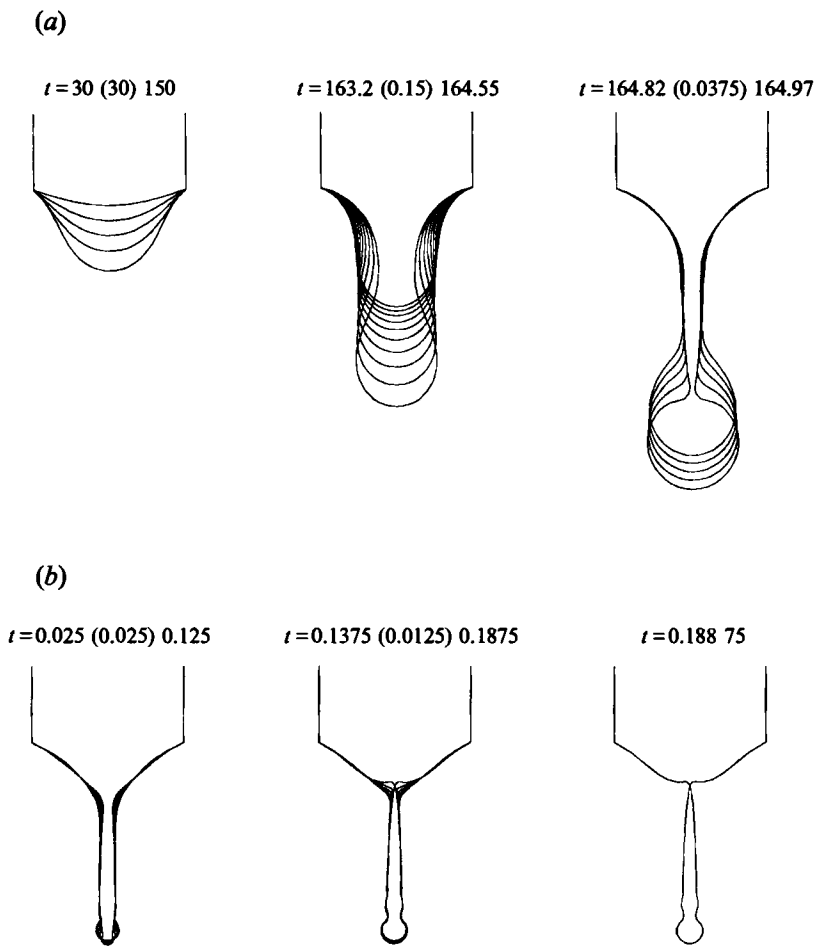

FIGURE 4. Plots of the free-surface shapes of the pendant drop during different stages of the evolution, (*a*) before and (*b*) after, the bifurcation. The Bond number is $Bo = 4$ and the discharge rate is $\mathcal{Q} = 0.01$.

Eventually a second bifurcation occurs with the volume of the secondary drop being $V_2 = 2.33$. The secondary drop has a volume which is almost 40% of the volume of the primary drop. This is in contrast to the case with $\mathcal{Q} = 0.01$ where the secondary drop had a volume less than 1% of that of the primary drop. The large difference in the volume of the drop after the second bifurcation is related to the fact that for $\mathcal{Q} = 0.01$ the secondary bifurcation occurred only 0.0725 time units after the first bifurcation. In contrast, for $\mathcal{Q} = 1.0$ the secondary bifurcation occurred 2.54 time units after the first bifurcation. Hence, for $\mathcal{Q} = 1.0$ the second bifurcation can be regarded as a bifurcation entirely separated from the primary bifurcation while for $\mathcal{Q} = 0.01$ the primary and secondary bifurcations are intimately linked.

Before we proceed to assess the effect of the Bond number on the evolution of the drop, let us briefly reconsider figures 2 and 3. We observe in figure 2 that after the second bifurcation one is left with a conical region which is rounded at the tip. In figure 3 we find that after the first bifurcation the fluid region is also distinctly conical with a rounded tip. Hence, under significantly different circumstances the bifurcation dynamics of a drop may, at some stage, result in the formation of a conical fluid region.

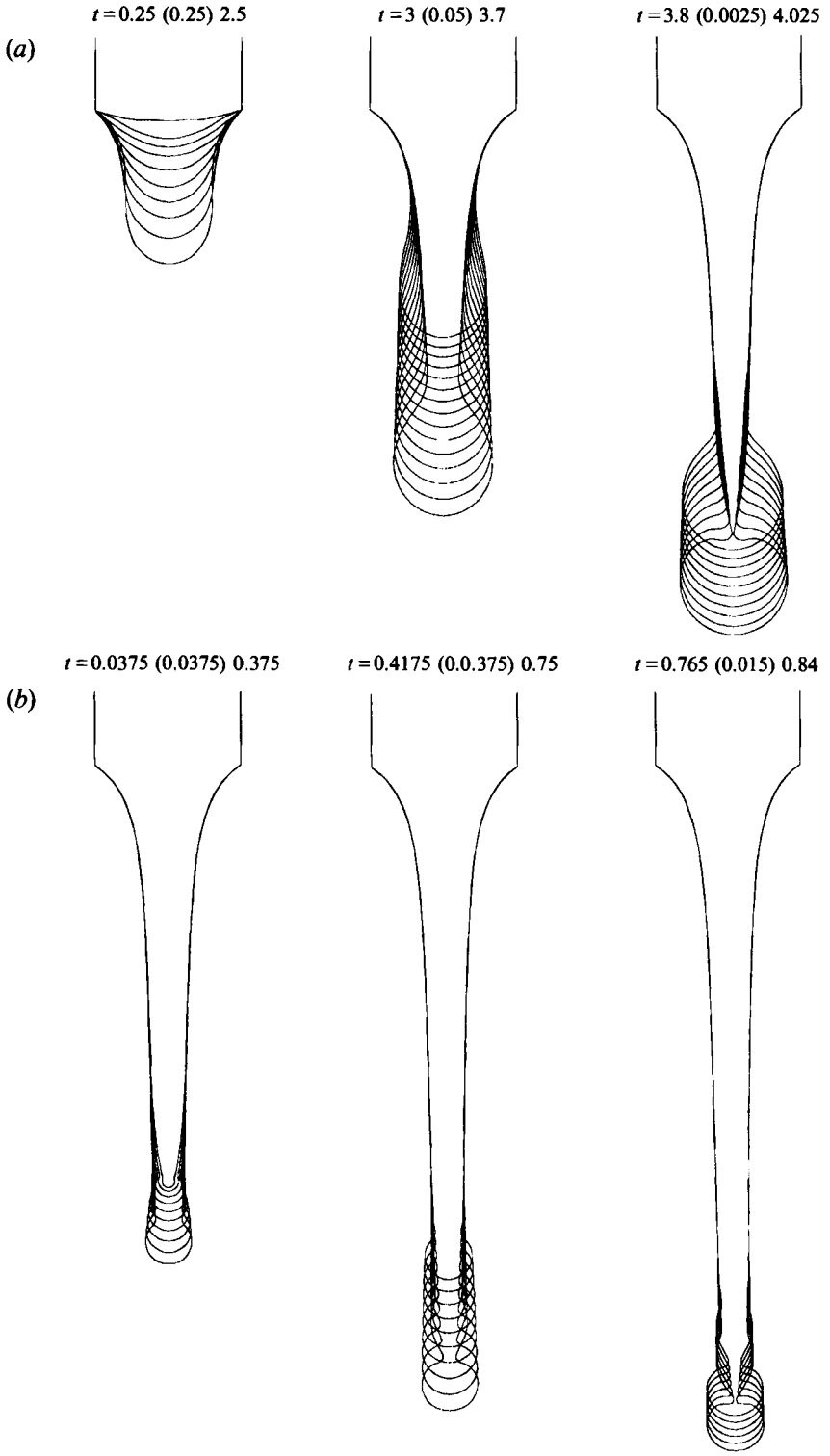

FIGURE 5. Plots of the free-surface shapes of the pendant drop during different stages of the evolution, (*a*) before and (*b*) after, the bifurcation. The Bond number is $Bo = 4$ and the discharge rate is $\mathcal{Q} = 1.0$.

An idea of how a fluid cone evolves under the action of surface tension forces may be obtained from the work by Keller & Miksis (1983) who showed that the evolution of a two-dimensional fluid wedge was self-similar. When this work is extended to the axisymmetric case, the self-similar character of the evolution of the cone is preserved (A. C. King 1993, private communications). When we go back to figure 3(*b*) we observe what appears to be a degree of self-similarity immediately after the bifurcation. Self-similarity is, however, destroyed by dynamic effects related to the bifurcation. In the Appendix we present some calculations of the evolution of conical fluid regions which are at rest initially. These calculations strongly suggest that the evolution of the fluid cone is self-similar. This implies that on very small time- and lengthscales the evolution of the fluid surface immediately after the bifurcation may be self-similar.

In order to assess the effect of the Bond number on the evolution of the drop we will now consider the case in which $Bo = 4$. As in the case with $Bo = 1$ we study the evolution for the discharge rates $\mathcal{Q} = 0.01$ and 1. First consider the evolution of the drop for the parameters $Bo = 4$ and $\mathcal{Q} = 0.01$ as depicted in figures 4(*a*) and 4(*b*), before and after the first bifurcation respectively. As in the case with $Bo = 1$ and $\mathcal{Q} = 0.01$ we observe that during the initial stage of the evolution, the drop grows only slowly. Once the critical volume is exceeded we see that the evolution speeds up significantly as the bifurcation point is approached. There are a number of noteworthy differences between the present case and the case with $Bo = 1$ (figure 2*a*). Clearly, the size of the drop relative to the radius of the nozzle has decreased significantly. Also, with $Bo = 4$ the length of the liquid bridge connecting the drop to the nozzle is much longer than for $Bo = 1$ and the conical surface between the liquid bridge and the nozzle is no longer as evident with $Bo = 4$ as it was with $Bo = 1$. Following the bifurcation (figure 4*b*) we observe essentially the same behaviour as in that depicted in figure 2*b*. The liquid bridge contracts owing to the large curvature at the tip and a bulbous end forms at the tip. After some time a secondary bifurcation occurs resulting in the satellite drop. The volume of the main drop was found to be $V_1 = 0.935$ while the secondary drop had a volume of $V_2 = 0.059$. Note that the volume of the satellite drop is approximately 6% of that of the main drop while in the case with $Bo = 1$ the satellite drop had a volume which was less than 1% of that of the main drop.

Increasing the volume flux to $\mathcal{Q} = 1$ the evolution of the drop before and after the bifurcation is as depicted in figures 5(*a*) and 5(*b*) respectively. As in the case with Bo $= 1$ and $\mathcal{Q} = 1$ we find here that the liquid bridge has been replaced by a slender liquid cone. Changes to the free surface immediately prior to the bifurcation (figure 5*a*) are confined to the tip of the cone and the spherical drop. Following the bifurcation (figure 5*b*) we observe that the evolution is distinctly different from that depicted in figure 3(*b*). Now we find that the tip of the liquid cone contracts only briefly. Subsequently the tip of the cone starts to descend while the small drop slowly develops at the end of the cone. The length of the cone grows significantly before the small drop eventually breaks away. The volume of the first drop was $V_1 = 1.63$ while that of the second drop is $V_2 = 0.22$. It is interesting to note that after the first bifurcation the fluid domain changes only at the tip of the fluid cone. The region immediately below the nozzle appears to be steady, unaffected by the downstream bifurcation.

5. Discussion

In the previous section we have seen that the volume of the drop following the first bifurcation is strongly dependent on the Bond number and the volume flux. In particular, we saw that the drop volume V_1 decreased with increasing Bond numbers

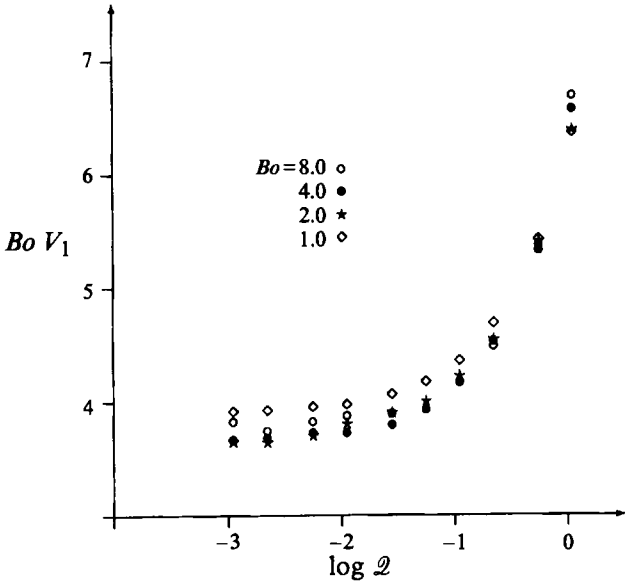

FIGURE 6. A plot of $Bo\,V_1$ versus $\mathcal{2}$. V_1 is the volume of the fluid region below the bifurcation point. The different symbols correspond to the Bond numbers indicated in the plot.

while V_1 increased with increasing volume flux. Let us now consider this dependence of V_1 on Bo and $\mathcal{2}$ in some more detail. In figure 6 we have plotted $Bo\,V_1$ versus $\log \mathcal{2}$ for the Bond numbers indicated in the plot. We note that while there is some variation, the scaled drop volumes for different Bond numbers are grouped fairly close together for a given value of $\mathcal{2}$. This implies that for a fixed volume flux we have roughly $V_1 \propto Bo^{-1}$. We observe that for $\mathcal{2} < 0.01$ the volume of the primary drop is almost independent of the volume flux. The reason for this is that for small volume fluxes the evolution of the drop, before the critical volume is exceeded, can be regarded as a succession of static drop shapes. Hence, at the critical volume the domain is only slightly modified by dynamic effects when the volume flux is small so that the evolution of the surface prior to the bifurcation is independent of the volume flux.

One could try to estimate the volume of the primary drop by taking an approach similar to that in the theory on the growth and detachment of bubbles from a nozzle. Assuming that for a slowly growing drop ($\mathcal{2} \ll 1$) immediately prior to the bifurcation the shape of the fluid region attached to the nozzle is spherical, one finds that surface tension and gravitational forces are in balance when the radius of the drop is equal to (see Fritz 1935)

$$R_d = \left(\frac{3\sigma R}{2\rho g}\right)^{1/3}.$$

If most of this fluid sphere were to break away from the nozzle, the dimensionless volume of the corresponding drop would be $V_d = 2\pi/Bo$. Hence, the scaled volume is then equal to

$$Bo\,V_d = 2\pi,$$

which is, in fact, an alternative statement of what is known as Tate's law. It is clear from figure 6 that this is a poor approximation of the actual volume of the primary drop. The reason why Tate's law is a poor approximation lies in the assumption that the fluid region attached to the nozzle is spherical and that most of the spherical

volume actually breaks away from the nozzle. In the previous section we saw that this is a very poor approximation indeed. This is in marked contrast to the situation in which a gas bubble breaks away from a submerged nozzle. In that case the bubble is approximately spherical when the bubble is small enough so that Tate's law gives a satisfactory approximation of the volume of the gas bubble (cf. Oğuz & Prosperetti 1993).

It is imperative to validate our numerical work by comparing results of our calculations with available experimental work. We start with a qualitative comparison of our calculations with the photographs presented by Peregrine *et al.* (1990). While a sequence of photographs of the evolution before and after the bifurcation is presented by Peregrine *et al.* (1990), it is not possible to compare our calculations with each of these photographs since the time separation between the photographs is not accurately known. However, during the evolution there are two well-defined time instances, namely the times at which the primary and secondary bifurcations occur. We will compare our numerical results with the photographs of Peregrine *et al.* (1990) at these time instances. We assume that in the experiments clean water was used which, together with the radius of the tube in the experiments of 2.6 mm, yields a Bond number of $Bo = 0.91$. In the experiments the drops were dripping 'as slowly as possible to minimize initial motion'. In our numerical calculations we take $\mathcal{Q} = 0.01$ which, as can be seen in figure 6, is in the regime in which the drop size is independent of the volume flux (for these parameters the first bifurcation occurred after approximately 540 dimensionless time units which corresponds to approximately 9 s). In figures 7(*a*) and 7(*b*) we show pictures of the experimental drop shapes at the first and secondary bifurcation points with the drop shape as obtained from our calcluations superimposed (the thin drawn line). We observe in figure 7(*a*) that there is a satisfactory agreement between our calculations and the experimental result. Two points at which the numerical and experimental results can be distinguished clearly are the transition regions between fluid cone and the liquid filament and the drop and the filament. In particular we observe that the top of the drop is somewhat dented in the numerical simulation whereas in the experiment the drop appears almost spherical. Also, the transition from the fluid cone to the filament is sharper in our calculations than in the experiment and we notice a slight asymmetry in the experiment. When we consider figure 7(*b*) we see that the agreement between the numerical result and the experiment is rather poor. Unfortunately, the slight asymmetry which is apparent in figure 7(*a*) is magnified substantially after the first bifurcation leading to a large asymmetry when the second bifurcation occurs. We notice, furthermore, that more undulations are visible on the filament in the experiment than on the calculated filament. This difference is likely to be due to the fact that with the number of grid points we have used we are not able to resolve these short-wavelength features. Notwithstanding the differences, we note that the contraction and flattening of the fluid cone is fairly well predicted by the calculations although the flattening of the cone is somewhat more in our computational results than in the experiment.

One of the applications of measuring the volume of fluid breaking away from a nozzle concerns surface tension measurements. Tables in which the volume of the drop breaking away from the nozzle is related to the coefficient of surface tension were published by Harkins & Brown (1919) for the case of low-viscosity liquids. It is important to emphasize that the drop volumes measured in experimental studies comprise the added volumes of the primary and secondary drops. Hence, if one aims to calculate drop volumes and compare these volumes with the experimental results, one is forced to proceed beyond the first bifurcation point. A good test of our

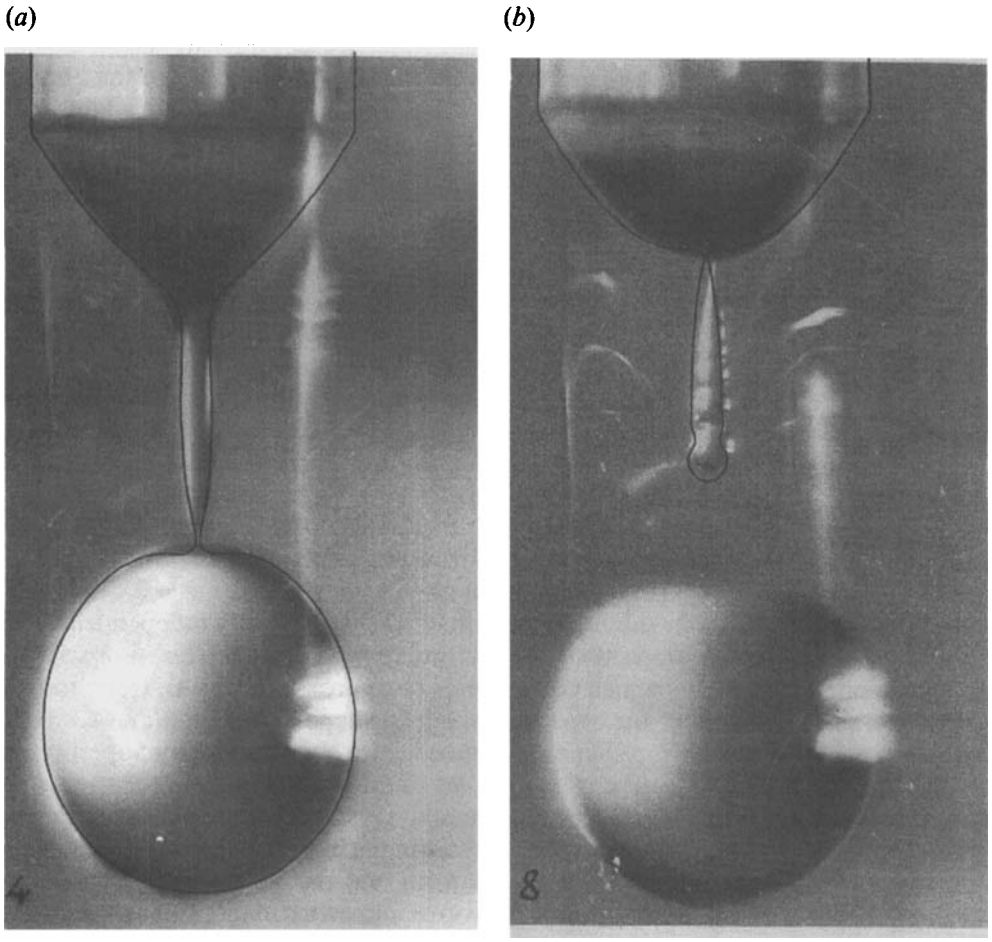

FIGURE 7. A comparison of experimental and calculated drop shapes at the instant of (*a*) the first and (*b*) the second bifurcation. The parameters used in the numerical simulation are $Bo = 0.91$ and $\mathcal{Q} = 0.01$. The photographs of the drops were supplied by Professor D. H. Peregrine.

numerical work, and in particular the validity of the approximation near the bifurcation point, is to compare drop volumes calculated numerically with those found experimentally by Harkins & Brown (1919).

In their experimental work, Harkins & Brown also investigated the effect of the rate of formation of the drop on the drop volume. They found that if the growth rate of a clean water drop on a tip with a radius of 0.245 cm (with corresponding Bond number $Bo = 0.82$) was such that a bifurcation occurred in less than 80 s, the weight of the fluid region breaking away was affected. Slower growth rates yielded approximately similar drop weights. Assuming a surface tension coefficient equal to that of clean water, we find that if we take $\mathcal{Q} = 0.001$ a bifurcation occurs in our calculations after approximately 90 s when $Bo = 1.0$ and 66 s when $Bo = 7$ (the capillary timescale T is related to the Bond number via $T = Bo^{3/4}(\sigma/\rho g^3)^{1/4}$). Given that dynamic effects during the evolution of the drop are very small for $\mathcal{Q} = 0.001$ we adopt the following procedure to reduce the computational time. For a given Bond number we calculate the static shape of the drop with a volume slightly less than the critical volume. We then start the calculation with the static shape as the initial configuration.

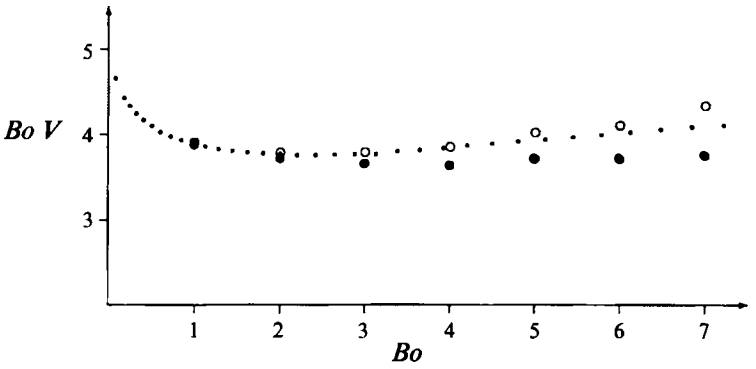

FIGURE 8. A plot of scaled drop volumes versus *Bo*. The curve of small dots corresponds to the experimental results obtained by Harkins & Brown (1919, table VIII), the circles are numerical results. The close circles correspond to the scaled drop volumes of the primary drop ($Bo\,V_1$) and the open circles are the scale volumes of the primary and secondary drops added together ($Bo(V_1+V_2)$).

Note that the procedure adopted by Harkins & Brown (1919) was essentially aimed at producing a static drop with a volume equal to the critical volume in order to eliminate dynamic effects related to the formation of the drop.

In figure 8 we have plotted the experimental results obtained by Harkins & Brown (1919) (the curve of small dots) and the drop volumes obtained from our numerical work. The closed circles are scaled volumes of the primary drop and the open circles are scaled volumes of the primary and secondary drops added together. We observe that our numerical results agree well with the experimental results when $Bo \leqslant 6$. For larger Bond numbers the calculated drop volumes deviated significantly from the experimental results. The differences between the experimental and numerical results may be due to discretization errors, our treatment of the necking region, viscous effects in the experiment or the fact that in the experiment the tip of the tube at which the drop formed was flat rather than the sharp-rimmed tip we have assumed in our calculations. We should, however, point out that the apparent reduction in accuracy of our calculations for $Bo > 6$ may be due, at least partly, to measurement errors in the experiment. Namely, the very careful experiments by Harkins & Brown (1919) yielded results accurate to less than 0.1% for $Bo < 6.5$ but for $Bo > 6.5$ Harkins & Brown indicated that the accuracy of their experiments reduced significantly. Interesting in this respect is the fact that we found the dynamics close to the bifurcation point to become increasingly violent for increasing Bond numbers. For example, whereas for Bo $\sim O(1)$ instabilities would not occur within 5 time steps (with $\Delta t = 0.01$) after the threshold neck radius $R_n = 0.02$ was exceeded, for $Bo > 6$ the instabilities would often occur within 2 time steps. This indicates a much more rapid and violent contraction of the neck for the larger Bond numbers.

When we consider the relative contributions of the primary and secondary drops to the volume breaking away from the nozzle, it is clear from figure 8 that for $Bo < 2$ the volume of the secondary drop is only a small fraction of the volume of the primary drop: the volume of the secondary drop is less than 2% of the volume of fluid breaking away from the nozzle. This situation changes dramatically when the Bond number increases; for $Bo = 7$ more than 10% of the fluid breaking away from the nozzle is taken up by the secondary drop. In table 1 we have listed the calculated volumes of the primary and secondary drops and the ratio of these volumes for different Bond numbers.

Bo	V_1	V_2	V_2/V_1
1	3.880	0.024	0.006
2	1.859	0.035	0.019
3	1.220	0.043	0.035
4	0.910	0.053	0.058
5	0.743	0.062	0.083
6	0.618	0.067	0.108
7	0.536	0.084	0.156

TABLE 1. Volumes of the primary and secondary drops and their ratio, calculated with $\mathcal{Q} = 0.001$ and various Bond numbers

6. Conclusions

In this paper we have shown that it is possible to calculate the evolution of a pendant drop until close to the bifurcation point. Owing to the singular nature of the bifurcation point we experience severe numerical difficulties when this point is approached. It is, however, possible to continue the calculation beyond the bifurcation point by modifying the free surface in the necking region once the radius neck has decreased sufficiently.

For small Bond numbers and for small growth rates we find that immediately prior to the first bifurcation, the fluid region had three distinct sections: a conical region connects a thin liquid filament to a spherical drop. First the spherical drop breaks away and shortly thereafter a second bifurcation occurs at the point where the liquid filament is connected to the cone. By increasing the Bond number we find that the conical region disappears and both the length and the radius of the liquid filament grow. Again, we find that after the spherical drop breaks away a secondary bifurcation occurs on the liquid filament. Owing to the increased size of the liquid filament, the volume of the secondary drop has increased as compared with the case for the smaller Bond number.

Increasing the discharge rate when the Bond number is small leads to the merging of the conical region and the liquid filament. Now we find that a long cone connects the drop to the nozzle. The first bifurcation is not succeeded immediately by a secondary bifurcation because the liquid filament is no longer present. When eventually a second bifurcation occurs we find that the volume of the second drop is comparable to that of the first drop. A large discharge rate ($\mathcal{Q} \sim 1$) together with a large Bond number ($Bo \geqslant 4$) leads to the development of a more or less steady flow region connected to the nozzle. Drops break away from the end of this capillary surface.

A qualitative and quantitative comparison of our calculations with experimental results shows a satisfactory agreement. The contraction of the liquid filament and the subsequent formation of undulations on the capillary surface are interesting details of our numerical calculations which are confirmed in experiments. Drop volumes breaking away from a nozzle have been calculated and are in good agreement with experimental measurements for Bond numbers $Bo \leqslant 6$. Our calculations show that the size of the secondary drop decreases relative to the size of the primary drop for decreasing Bond numbers, i.e. as the Bond number decreases an ever larger fraction of the volume breaking away from the nozzle is taken up by the primary drop. We are not aware of experimental results which confirm this observation.

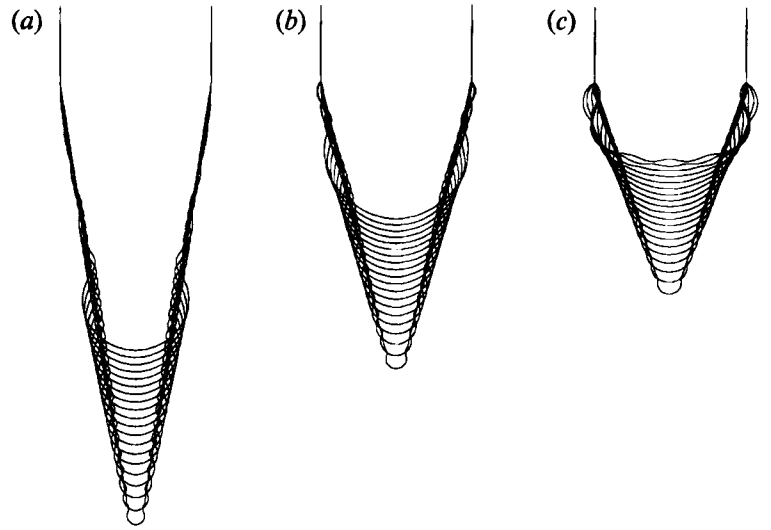

FIGURE 9. Plots of the free-surface shapes of a contracting liquid cone: (*a*), (*b*) and (*c*) show the evolution of cones with semi-angles equal to $\theta = 0.05\pi$, 0.075π and 0.1π respectively. In all three figures the free-surface shapes are shown at times $t = 0.05\,(0.05)\,1.0$.

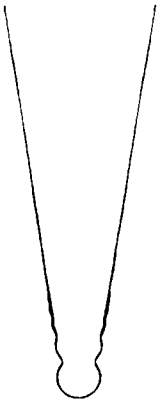

FIGURE 10. The free-surface shapes of the evolving cone for the case with $\theta = 0.05\pi$ at the times $t =$ 0.25, 0.5, 0.75 and 1.0. The free-surface shapes at the different times are superimposed, appropriately scaled and shifted to exhibit the self-similar character of the evolution.

Appendix

Here we will present some results of calculations concerning the evolution of a fluid cone driven by surface tension forces. It is assumed that the fluid cone is at rest initially and we take $Bo = \mathcal{Q} = 0$. The conical region is taken to have a base with unit radius while at the tip of the cone we place a spherical cap with radius r_T. The semi-angle of the cone is denoted by θ. In figure 9(*a–c*) we have plotted different stages of the evolution of a cone with $r_T = 0.05$ and $\theta = 0.05\pi$, 0.075π and 0.1π respectively. All the free-surface shapes in figure 9 are shown at equal time intervals. In all cases we observe that the fluid cone contracts in a regular manner until the point at which disturbances on the capillary surface reach the contact line of the fluid cone and the rim of the nozzle. To investigate the possible self-similar character of the evolution of the cone as shown in figure 9, we can superimpose appropriately shifted and scaled free-surface shapes to determine whether or not the surface shape changes with time. The free-

surface shapes as shown in figure 9(*a*) at the times $t = 0.25, 0.5, 0.75, 1.0$, scaled and shifted (the scaling factors for the subsequent times are 1.0, 0.645, 0.488 and 0.417 respectively) are plotted in figure 10. We observe that the free-surface shapes are indeed self-similar. Self-similarity is destroyed eventually owing to the finite extent of the domain. Extending our investigation to self-similarity for very short times is limited by the resolution of our numerical scheme. It is interesting to note that a log–log plot of the scaling factors versus time reveals that the rate at which the tip of the cone contracts is proportional to $t^{-0.63}$. This is close to the value $t^{-2/3}$ as obtained by Keller & Miksis (1983) in their study of a contracting liquid wedge.

REFERENCES

EGGERS, J. 1993 Universal pinching of 3D axisymmetric free-surface flow. *Phys. Rev. Lett.* **71**, 3458–3460.

EGGERS, J. & DUPONT, T. F. 1994 Drop formation in a one-dimensional approximation of the Navier–Stokes equation. *J. Fluid Mech.* **262**, 205–222.

FRITZ, W. 1935 Berechnung des maximale Volume von Dampfblasen. *Phys. Z.* **36**, 379–384.

GUTHRIE, C. 1863 *Proc. R. Soc. Lond.* **8**, 444.

HARKINS, W. D. & BROWN, F. E. 1919 The determination of surface tension (free surface energy) and the weight of falling drops: The surface tension of water and benzene by the capillary height method. *J. Am. Chem. Soc.* **41**, 499–524.

HAUSER, E. A., EDGERTON, H. E., HOLT, B. M. & COX, J. T. 1936 The application of the high-speed motion picture camera to research on the surface tension of liquids. *J. Phys. Chem.* **40**, 973–988.

KELLER, J. B. & MIKSIS, M. J. 1983 Surface tension driven flows. *SIAM J. Appl. Maths* **43**, 268–277.

LEE, H. C. 1974 Drop formation in a liquid jet. *IBM J. Res. Dev.* **18**, 364–369.

OĞUZ, H. N. & PROSPERETTI, A. 1993 Dynamics of bubble growth and detachment from a needle. *J. Fluid Mech.* **257**, 111–145.

PADDAY, J. & PITT, A. R. 1973 The stability of axisymmetric menisci. *Phil. Trans. R. Soc. Lond.* A **275**, 489–528.

PEREGRINE, D. H., SHOKER, G. & SYMON, A. 1990 The bifurcation of liquid bridges. *J. Fluid Mech.* **212**, 25–39.

RAYLEIGH, LORD 1899 Investigations in capillarity. *Phil. Mag.* **48**, 321–337.

SCHULKES, R. M. S. M. 1993 Nonlinear dynamics of liquid columns: a comparative study. *Phys. Fluids* A **5**, 2121–2130.

SCHULKES, R. M. S. M. 1994 The evolution of capillary fountains. *J. Fluid Mech.* **261**, 223–252.

TATE, T. 1864 On the magnitude of a drop of liquid formed under different circumstances. *Phil. Mag.* **27**, 176–180.

TING, L. & KELLER, J. B. 1990 Slender jets and thin sheets with surface tension. *SIAM J. Appl. Maths* **50**, 1533–1546.

WORTHINGTON, A. M. 1881 *Proc. R. Soc. Lond.* **32**, 362.